Assessment of the transverse roughness of the thin-walled cooler for the robot control system made using CAM programming

Peter Tirpak[1,], *Peter* Michalik[1,*], *Michal* Hatala[1], and *Michal* Petruš[1]

[1]Technical University of Kosice, Faculty Manufacturing and Technologies, with seat in Presov, 08001, Sturova 31, Slovakia

Abstract. The article deals with design and design of a thin-walled heat sink for the robot control system, the measurement of the transverse roughness of the touch surfaces and the programming procedure in Autodesk Inventor 2019 software. In this software, a design of the 3D model of the heat sink generated based on power supply and NC code generation for the Fanuc control system. The production it-self carried out on the CNC Vertical Machining Center Pinnacle 2100 with this control system. The longitudinal surface roughness was measured with a Mitutoyo SJ 400 dredger and the measurement result was the maximum Ra = 0.69 μm and Rz = 4.1 μm.

1 Introduction

Processor manufacturers for robot control systems are constantly increasing their performance, which greatly affects the way they cooled.

Fig. 1. Passive cooler. Source: [17]

* Corresponding author: peter.michalik@gmail.com

The first processors did not need special cooling, but with the increasing power of the processors, the coolers adapted it, either by size or by choosing a different type of material for their production. At present, coolers used passively and actively. The characteristic feature of the passive cooler (Fig. 1) is the ribbed and its base attached to the processor. Frequently used aluminium or alumina slowly extruded with copper, which has better thermal conductivity. With the active heatsink, a fan for the passive cooler rib added. The fan blows the air between the ribs to increase cooling efficiency. The disadvantage of this type of heat sink is the risk of damaging or destroying the fan and this result in the processor destroyed by its rising temperature. Depending on the use of bearings, we distribute fans on fan bearings that are less expensive but more susceptible to failure and fan bearings that are of better quality (Fig. 2).

Fig. 2. Active cooler. Source: [17]

The heat-conducting paste that fills the microscopic inequalities and thus maximizes heat transfer from the body to the chiller also plays an important role. The heat conducting paste applied to the entire surface of the processor and is then fit-ted with a cooler. Active coolers mostly used to cool high-power processors where passive coolers are no longer sufficient. In addition to air-cooling, it is also possible to use water cooling, cooling with nitrogen or Peltier cells. These types of cooling are more efficient than air-cooling, but they are structurally more complex, so they are not common. With Peltier cooling, an additional cooling cooler needed to cool Peltier itself, which is an energy disadvantage, but this article can produce extremely low temperatures. Most electronic components, including the processor, emit heat when it turned on. This heat is undesirable for the entire robot control system, and therefore an additional auxiliary fan installed in the entire box. Another fan also contains a power supply. The auxiliary fan ensures continuous air circulation in the control cabinet. The incoming air from the bottom of the cabinet cools down the entire circuit gradually, and as it gradually heats the rising of the mountain and fed by the fan of the source. The "chimney effect" used here [17]. Michalik et al. [1-2] dealt with surveying the surface quality of the thin-walled parts of the C45 steel rod. Milling of thin-walled parts and evaluation of machining quality for the aerospace industry dealt with by Meshreki [3]. Kuram et al. and Miko et al. [4, 5] performed the prediction of the treatment of machined thin-walled parts. The wear of cutting material during the C45 steel evaluated by Duplak et al. [6], Fedorko et al. [7-8]. Lehocka et al. [9] performed comparison of the quality of the sur-face quality of the various materials in the aqueous stream treatment. Selected diagnostic methods for assessing the condition of the gearbox of machining center accrued from collaboration applied Baron et al. [10]. CAM programming for the production of thin-

walled components was applied by Fabian et al., Michalik et al., Kral et al., Mantic et al., Peterka et al. [11-16].

2 Manufacturing diagram and machined materials

Dimensions for the thin-walled Fig. 3 cooler matched to the processor and the cooling system itself. The contact surface of the radiator was 40 x 40mm.

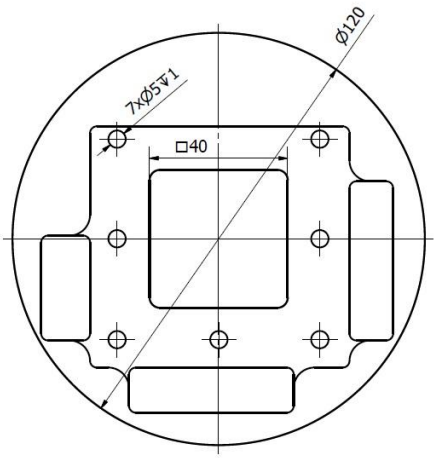

Fig. 3. Manufacturing diagram of thin-walled cooler.

The material AlCu4PbMgMn chosen for the production of the thin-walled cooler. The elements, which contain this material, described in Table 1. The selected semi fabric was a circular rod with a diameter of 120 mm.

Table 1. Data of material AlCu4PbMgMn.

AlCu4PbMgMn										
Element	**Si**	**Fe**	**Cu**	**Mn**	**Mg**	**Cr**	**Ni**	**Zn**	**Ti**	**Pb**
Content element [%]	0,80	0,80	3,3	0,5	1,8	0,10	0,20	0,80	0,20	1,5

The milling tool used with a diameter of 12 mm and clamped into a short clamp holder using a pinch of Fig. 4. The tool speed was 1200 minutes and a feed rate of 600 millimetres per minute.

Fig. 4. Short clamping thorn for milling tool.

3 Programming of cooler manufacturing

Autodesk Inventor 2019 software created the NC program code. After the model was loaded, the zero point of the component Fig. 5 selected first.

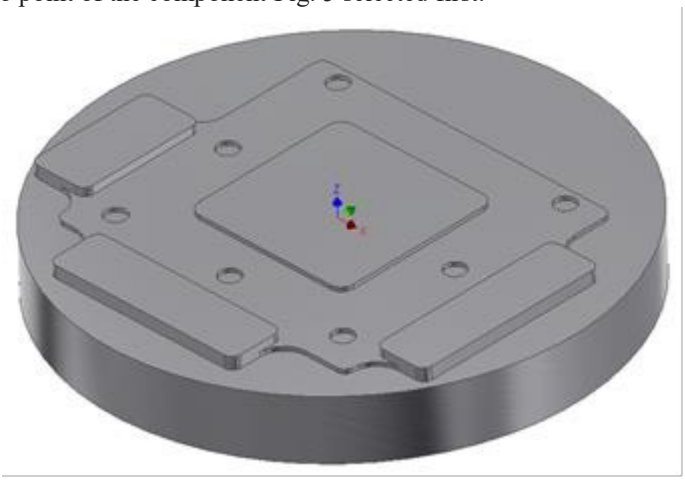

Fig. 5. Selection position of coordinate system.

The tool selection and setting of the cutting conditions Fig. 6 followed.

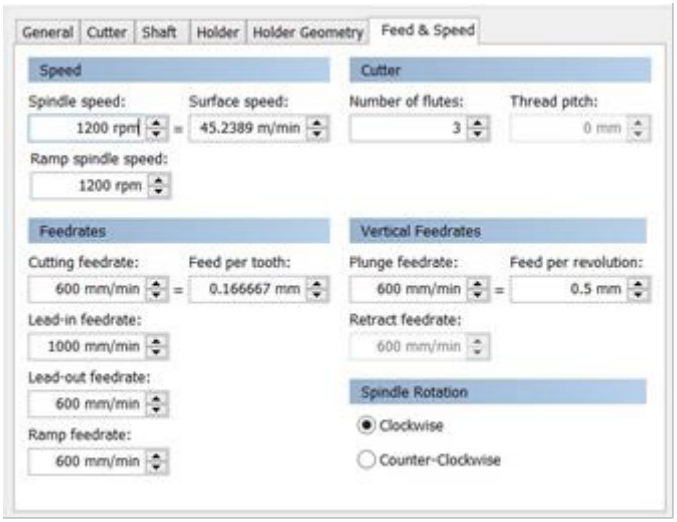

Fig. 6. Selection cutting tool and cutting conditions.

The component made with an addition of 0.2 mm. The milling tool was a Ø 12 mm cutter with four cutting plates. After selecting the tool and entering its cutting conditions, simulation of the coincidence Fig. 7 and finishing of Fig. 8 followed.

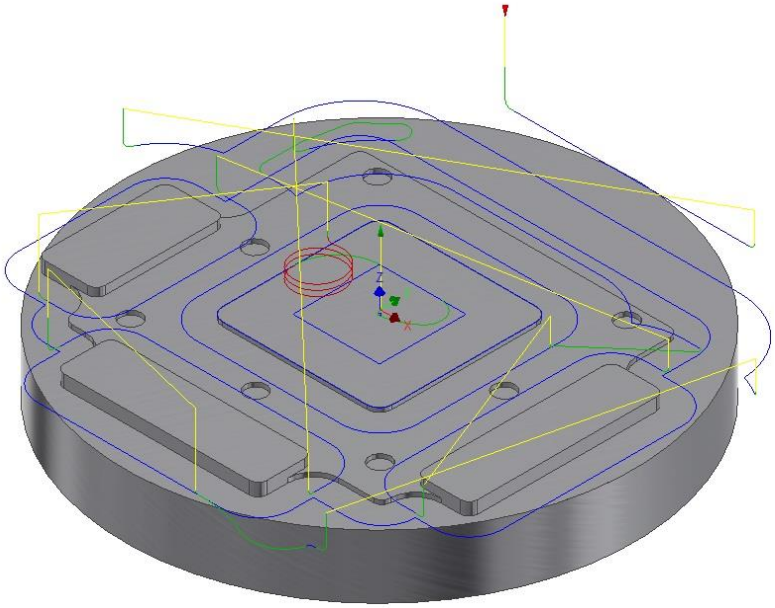

Fig. 7. Simulation of roughing machining.

Fig. 8. Simulation of finishing machining.

4 Machining and measuring thin-walled cooler

The production of the thin-walled cooler carried out at the Pinnacle 2100 Vertical CNC Machining Centre, using the Fanuc control system (Fig. 9).

Fig. 9. Machining tin-walled component on the vertical CNC milling centre Pinnacle 2100.

The semi-finished product for the thin-walled cooler clamped in the three-piece chuck at the work centre desk of the machining centre. Using the Mitutoyo SJ 400 Fig. 10, the transverse roughness of the contact surface of the radiator measured.

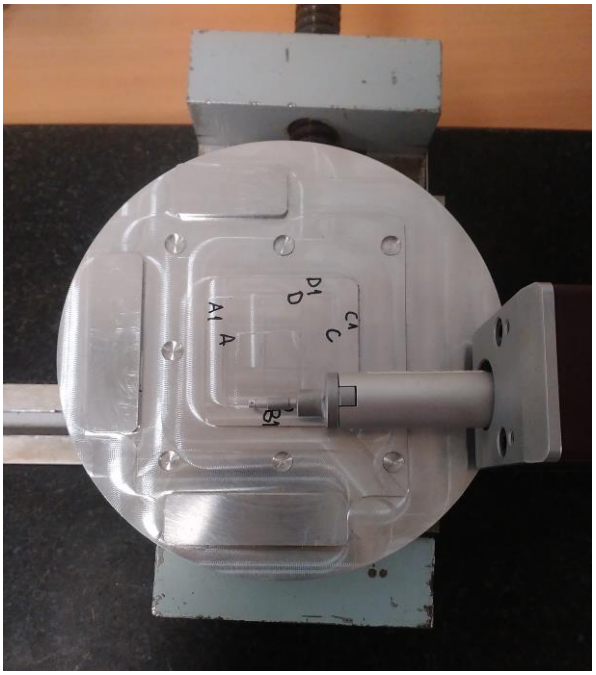

Fig. 10. Measurement trnasverse roughness by device Mitutoy SJ 400.

On the contact surface of the radiator, the toolbar paths A were marked; B; C; D; A1; B1; C1; D1. The measurement was performed at the indicated locations, repeated ten times, and the resulting Ra and Rz values were recorded in the tables from which the resulting roughness graphs in the A sites were created; B; C; D Fig. 11 and for A1 paths; B1; C1; D1 Fig. 12.

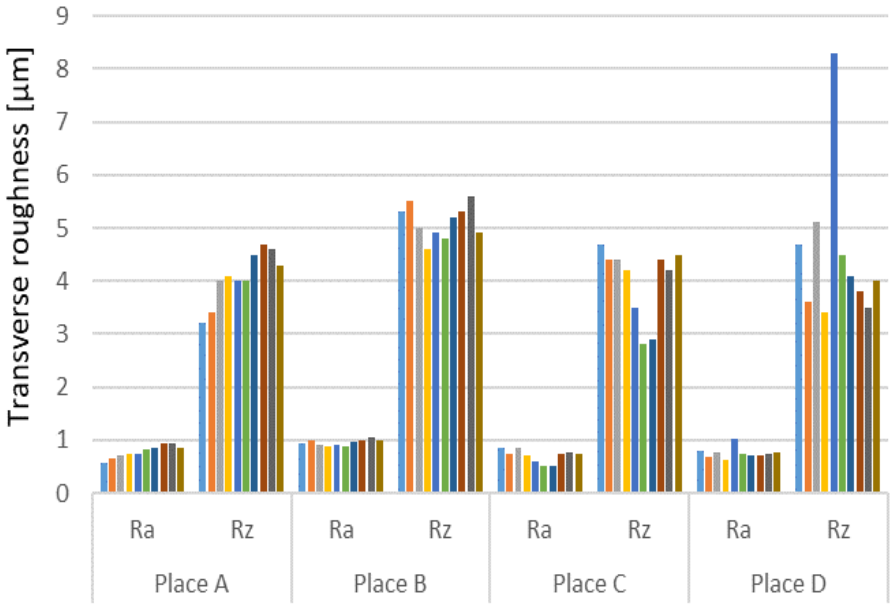

Fig. 11. Transverse roughness on the place A; B; C; D.

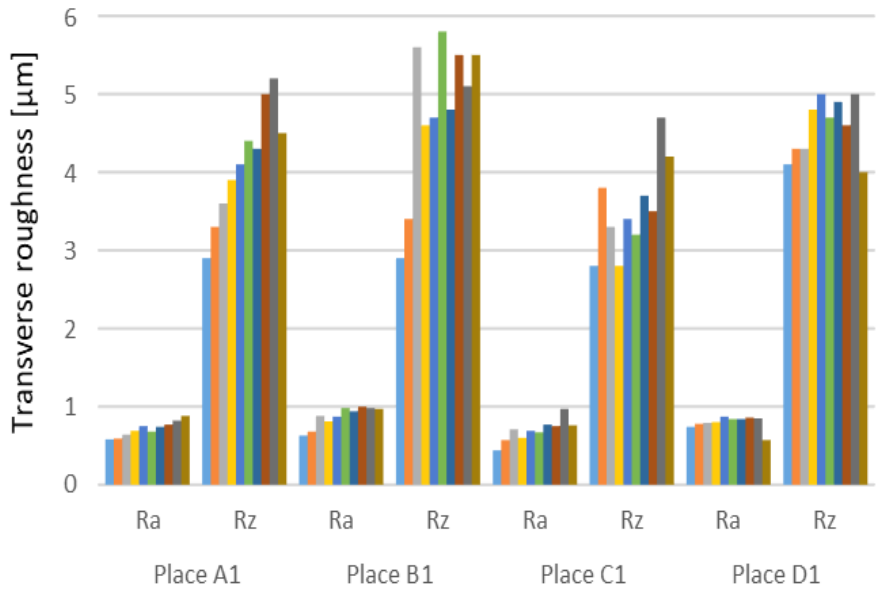

Fig. 12. Transverse roughness on the place A1; B1; C1; D1.

5 Conclusion

Today they used in pipe coolers. There is a special fluid in these copper tubes. These tubes deliver heat from the processor to the heat sink. The liquid in the tubes is self-circulating thanks to the physical demise. The more tubes are in the cooler, the cooling is more efficient. Because of the roughness measurement, the lowest roughness value Ra = 0.44 μm, Rz = 2.8 μm was measured at the location A1. The maximum value Ra = 1.04 μm, Rz = 8.3 μm was measured at the location D.

This work is a part of research project VEGA 1/0045/18, VEGA 1/0492/16.

References

1. P. Michalik, J. Zajac, M. Hatala, D. Mital, V. Fecova, Measurement **58** (2014)
2. P. Michalik et al. Číslicovo riadené obrábacie stroje a ich programovanie, **1** (2015)
3. M. Meshreki, Dynamics of Thin-Walled Aerospace Structures for Fixture Design in Multi-axis Milling, **5** (2009)
4. E. Kuram, B. Ozcelik, Measurement **46** (2013)
5. E. Miko, L. Nowakowski, Procedia Eng. **39** (2012)
6. J. Duplák, A. Panda, M. Kormoš, I. Pandová, S. Jurko, Key Eng. Mater. **663** (n.d.)
7. G. Fedorko, V. Molnár, A. Pribulová, P. Futáš, D. Baricová, Met. 5 (2011)
8. G. Fedorko, V. Molnar, A. Grincova, M. Dovica, T. Toth, N. Husakova, V. Taraba, M. Kelemen, Eng. Fail. Anal. **39** (2014)
9. D. Lehocka, D. Klichova, J. Foldyna, S. Hloch, P. Hvizdoš, M. Fides, F. Botko, Measurement **110** (2017)
10. P. Baron, M. Kočiško, J. Dobránsky, M. Pollák, M. Telišková, Measurement **94** (2016)
11. M. Fabian, P. Ižol, D. Draganovská, M. Tomáš, Appl. Mech. Mater. **474** (2014)
12. P. Michalik, J. Zajac, M. Hatala, Adv. Sci. Lett. **19** (2013)
13. J. Kral, et al., , Acta Mech. Slovaca **5** (2008)
14. M. Mantic, J. Kulka, J. Krajnak, M. Kopas, Influence of selected digitization methods on final accuracy of 3D model, (2016)
15. P. Michalik, J. Zajac, J. Duplák, A. Pivovarník, Lect. Notes Electr. Eng. **141** (2011)
16. J. Peterka, L. Morovič, P. Pokorný, M. Kováč, F. Hornák, Appl. Mech. Mater. **421** (2013)
17. https://en.wikipedia.org/wiki/Computer_cooling